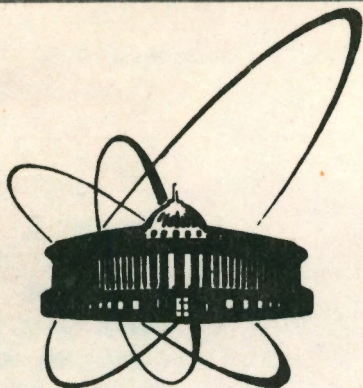


90-344



ОБЪЕДИНЕННЫЙ
ИНСТИТУТ
ЯДЕРНЫХ
ИССЛЕДОВАНИЙ
ДУБНА

К 74

E2-90-344

B.Z.Kopeliovich, L.B.Litov, J.Nemchik

EFFECTS OF FORMATION TIME
AND COLOUR TRANSPARENCY
ON THE PRODUCTION
OF LEADING PARTICLES OFF NUCLEI

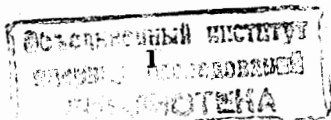
Submitted to "Zeitschrift für Physik C"

1990

1. Introduction

Nuclei supply us with an unique possibility of verifying of our ideas about the space-time pattern of strong interactions at high energies and properties of hadronic matter at the early stages of the scattering process. Apart from hadronic interactions where experimentators can observe only final products of the reaction at asymptotic distances, nuclei possess to make an unformed hadronic object to rescatter once more after its creation in a distance of about a few Fm. The most popular ideas examined in the particle-nucleus interactions are the concept of a final time of hadron formation, and recently the phenomenon of colour transparency, which is one of the most salient QCD predictions. The former was formulated first in the framework of the old parton model with short correlation in the rapidity scale. The formation length was considered to be rising proportionally to a hadron momentum. Later however, it has been shown^{1/} that in the string model and other QCD induced approaches the formation length does not rise, but tends to zero towards kinematic boundary. This effect gave rise to the nuclear shadowing in hadro-production of J/ψ ^{2/} and high- p_T production of symmetric hadron pairs on nuclei^{3/}. Analogous effects of enhanced nuclear shadowing near the edge of kinematical region should be observed also in soft reactions. The effects of nuclear colour transparency being in fact the widely known inelastic shadowing, make the nuclei as a rule more transparent in soft reactions also but not so considerably as in hard scattering.

In second and third sections of present paper we describe the eigen-state method of computation of inelastic corrections to the eikonal approximation and its realisation in an approach accounting for the colour dynamics of strong interaction. In the latter case we propose a novel variant of parameterization of the dependence of hadron interaction cross section on the relative



quark impact parameter, which nicely fits the experimental data on total hadron-nucleus cross sections. The concept of formation time is considered in section 4. It is found out that the result strictly depends on the topology of graphs in consideration. Even in the case of diffraction scattering where all valence quarks are spectators, the nuclear shadowing looks like that, as if a formation length would exist also. Section 5 contains some critique of the usage of the AGK cutting rules for determination of the weights of contribution of the manyparton components of the hadronic wave function to the inclusive production cross section. It is found preferable to suppose a target-independence of parton momentum distribution. Section 6 is devoted to numerical calculation of cross sections and to comparison with experimental data.

2. Inelastic corrections to the eikonal approximation

The basis for description of the high energy nuclear interactions is the Glauber-Sitenko approach^{4,5/} (GSA), which corresponds to the eikonal approximation. At high energies Gribov's inelastic shadowing^{6/}, corresponding to inelastic rescatterings (IS) shown in diag.1a, becomes important. The estimation of IS for heavy nuclei has been given in ref.^{7/}. The cross section σ_{tot}^{hN} is well described by diag.1a. due to the smallness of inelastic corrections. However, with the increasing of the experimental data precision and improving of the calculation technique we are faced with the necessity of consideration of higher order inelastic corrections as ones, represented on diag. 1b. The same problem takes place in the case of some specific nuclear reactions, in which IS become of the order of hundred percents.

In paper^{8/} the so-called eigenstate method^{9/} for calculation of the inelastic corrections in the case of hadron nucleus reactions has been developed and successfully used.

Let us remind the main idea of this method: Choosing an appropriate basis for interaction eigenstates $|k\rangle$

$$\hat{f} |k\rangle = f_k |k\rangle, \quad (1)$$

where \hat{f} and f_k are scattering-amplitude operator and its eigenvalues, the physical state $|h\rangle$ is given by

$$|h\rangle = \sum_k c_k^h |k\rangle, \quad (2)$$

where the coefficients c_k^h obey the following conditions

$$\sum_k c_k^h (c_h^g)^* = \delta_{hg}, \quad \sum_k c_k^h (c_l^h)^* = \delta_{lk}$$

Let us consider, for example, the case of hadron nucleus inelastic rescattering at sufficiently high energy ($E \gg R_A \cdot m_h^h$). In this case during the time when interaction takes place, different hadron wave-function eigenstates are not mixed, i.e. hadron fluctuations are "frozen". Then the eigenstate $|k\rangle$ amplitude may be calculated in GSA. Thus, the elastic amplitude at impact parameter b has the following form

$$f_{el}^{hA}(b) = 1 - \langle \exp[-f_k T(b)] \rangle, \quad (3)$$

where $T(b)$ is the nuclear profile function

$$T(b) = A \int_{-\infty}^{\infty} \tilde{\rho}(b, z) dz \quad (4)$$

$$\tilde{\rho}(b, z) = \frac{1}{2\pi B} \int d^2 b' \rho_A(b', z) \exp\left(-\frac{(b-b')^2}{2B}\right). \quad (5)$$

Here $\rho_A(r)$ is the nuclear matter-density (for point like nucleons) further used in the Wood-Saxon form^{10/}. In (2) B is the slope of the diffraction cone of the hN scattering. The distinction between (1) and GSA is that in the first case the whole exponential is averaged. The difference

$$\Delta_{in} = \langle \exp[-f_k T(b)] \rangle - \exp[-\langle f_k \rangle T(b)]$$

gives just the inelastic corrections to the GSA. This is equivalent to the counting of all possible intermediate states in the hadron basis^{9/}. The price, however, is that our calculations become model-dependent, because a change of the scattering amplitude eigenstates and eigenvalue spectrum leads to a change in the final result. The positive moment here is the possibility of probing different models.

There is a widespread confusion with identifying $\rho_A(r)$ with the charge distribution $\rho_{ch}(r)$, which incorporates the finite charge radius of the nucleon:

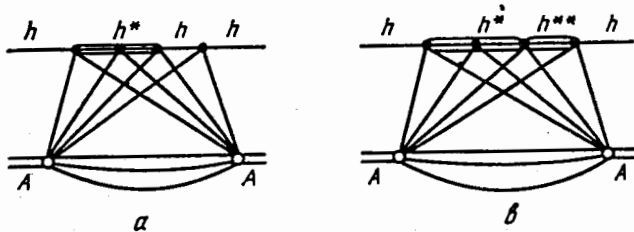


fig. 1. Graphs corresponding to the inelastic corrections.

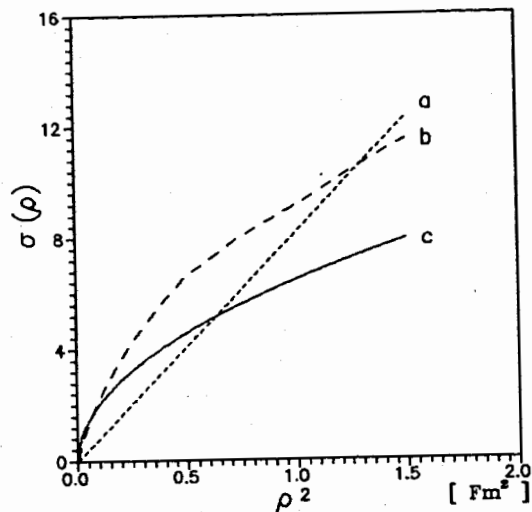


fig. 2. The total cross sections of $q\bar{q}$ pair interaction with a nucleon as a function of ρ^2 - the interquark relative impact parameter squared. The dotted and the solid curve correspond to parametrizations (9) and (11) respectively. The dashed curve corresponds to the two-gluon exchange approximation.

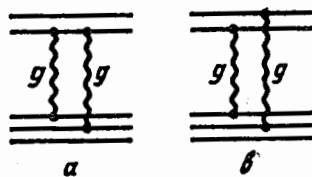


fig. 3. Contributions to the meson-nucleon elastic scattering amplitude (pomeron exchange in two-gluon approximation)

$$\rho_{ch}(r) = \int d^3r' \rho_A(r') [\rho_{ch}(r-r')]_N. \quad (6)$$

The usage of $\rho_{ch}(r)$ is much more convenient, as the Nuclear Data Tables^{/10/} cite parameters namely for $\rho_{ch}(r)$. Then one should make a correction for the charge radius of the proton and neutron in further calculation of $T(b)$ using equation (1)^{/11/}:

$$B \rightarrow B - \frac{1}{3} (\langle R_{ch}^2 \rangle + \langle R_{ch}^2 \rangle). \quad (7)$$

Renormalization (7) corresponds to a Gaussian form factor of the nucleons, being a rather good approximation for our purposes.

So, using optical theorem and (1) we get for the total hadron-nucleus cross section

$$\sigma_{tot}^{hA} = 2 \int d^2b \langle 1 - \exp \left[-\frac{1}{2} \sigma_{tot}^{hN} T(b) \right] \rangle. \quad (8)$$

We would like to emphasize that in (8) the inelastic corrections are included.

3. Colour screening effects

One of the most expressive consequences of the colour dynamics of hadronic interactions is the cross section vanishing for point-like hadron fluctuations. The hadrons which are colourless systems can interact only because the colour is distributed inside them. If the hadron transverse size ρ tends to zero, then the interaction cross section decreases as ρ^2 . This fundamental QCD consequence has been experimentally investigated in the quasi-free charge exchange reaction $\pi^-A \rightarrow \pi^0X$ at 40 GeV and in the $pA \rightarrow ppX$ quasielastic rescattering in energy region 6 - 13 GeV. The above processes at large Q^2 are suitable for this purpose because of the singling out small transverse-size hadron fluctuations thus ensuring the cross section behaviour $\sigma(\rho) \sim \rho^2$. The physical parameter determining the size of the region where $\sigma(\rho) \sim \rho^2$ depends on the concrete dynamics.

Let us consider several alternatives (depicted in fig.2):

1. The interaction cross section $\sigma(\rho)$ of the $q\bar{q}$ pair with a nucleon depends in a simplest way on the relative impact distance ρ .

$$\sigma(\rho) = \frac{\rho^2}{\langle \rho^2 \rangle_h} \sigma_{tot}^{hN} \quad (9)$$

We averaged over transverse size of the target nucleon. The averaging over ρ is carried out with weight factor $|\Psi_h(\rho)|^2$, $\Psi_h(\rho)$ being the hadron wave function. Note that $\sigma(\rho)$ is an universal quantity. It does not depend on the sort of the investigated hadrons and on the quark flavour. Moreover, we shall use relation (9) for NN scattering too, assuming that in the nucleon wave function predominates the component with a compact diquark, which has the same colour as the antiquark. The difference between σ_{tot}^{NN} and $\sigma_{tot}^{\pi N}$ is caused by the difference between $\langle \rho^2 \rangle_N$ and $\langle \rho^2 \rangle_\pi$.

Using (8) and (9) we can calculate the total hadron-nucleus cross sections. As is shown on fig.3, this parameterization leads to an overestimation of inelastic corrections, hence, to an underestimation of the experimental data^{/12/}.

2. Though the calculation of the total cross sections in the framework of the QCD perturbation theory is not established at all, it takes into account the colour-screening effects that manifest itself in cancellation of the contributions of graphs on fig.4a, 4b at $\rho \rightarrow 0$. From these graphs with massless gluons $\sigma(\rho)$ is obtained in the form

$$\sigma(\rho) = \frac{16\pi\alpha_s^2}{3\beta^2 \ln 2} [1 + C - e^{-\gamma} + \ln \gamma - (1+\gamma)Ei(-\gamma)], \quad (10)$$

where $\gamma = \beta^2 \rho^2 / 4$; $\beta \approx 3.2 \text{ fm}^{-2}$ and C is Euler constant. The constant α_s is determined by the condition

$$\sigma_{tot}^{\pi N} = (16/3)\pi\alpha_s^2/\lambda^2.$$

Neutron-nucleus total cross sections obtained with the help of (10) are in a better agreement with the experimental data as is seen from fig.3.

3. The QCD lattice calculations show, that the confinement radius, i.e. the distance where $\alpha_s(q^2) \approx 1$, is much smaller than the light meson radius. This allows one to assume that the colour field in the hadrons is located in tubes with a transverse size of about 0.1 - 0.3 Fm, i.e. much smaller than the longitudinal one^{/13/}. The valence quarks or diquarks are placed at the end-points of these tubes. In the case of inelastic scattering the interacting-hadron tubes intersect in the impact-parameter plane.

After interaction the tubes are restored, now connecting the target and beam quarks. From topology-classification point of view this corresponds to a cylinder-type graph, i.e. pomeron. The probability for the tube crossing is proportional to the tube's length, $\sigma(\rho) \propto \rho$, when $\rho \gg \rho_0$, ρ_0 being the transverse tube-size. When $\rho < \rho_0$, another relation takes place: $\sigma(\rho) \propto \rho^2$. Thus, it is natural to choose the following parameterization for $\sigma(\rho)$

$$\sigma(\rho) = \begin{cases} c\rho^2, & \rho < \rho_0 \\ c\rho_0\rho, & \rho > \rho_0 \end{cases} \quad (11)$$

Here parameter c is obtained from the condition $\langle \sigma(\rho) \rangle_h = \sigma_{tot}^{hN}$ and parameter ρ_0 provides a satisfactory description of the experimental data. It is natural to assume that ρ_0 has the same value for all hadrons. The result of calculation of σ_{tot}^{hN} with $\rho_0 = 0.1 \text{ Fm}$ is represented on fig.3. This version of $\sigma(\rho)$ parameterization gives the best description of the experimental data, which is not surprising because of the presence of a free parameter. The value of ρ_0 is in a good agreement with the theoretical expectation^{/13/}. Note that the high accuracy in description of experimental data on total hadron-nucleus cross sections is required because inelastic shadowing appear as a correction to a small exponential term as compared with unity in expression (8). For the processes subject of our further considerations this exponential enters the cross section as a general factor.

4. Formation length and colour string interactions in the nucleus

It is now well established from theoretical and experimental studies of hadron-nucleus collisions at high energies that hadrons are not produced at the moment of collision but only after some "formation" time. Let a quark with a momentum k is produced inside a nucleus at a point z (for example, in a lepton-nucleus deep inelastic scattering). It then propagates accompanied by a satellite diquark or antiquark, compensating its colour. The string stretched between them is successively broken by $q\bar{q}$ -pairs tunneling from vacuum. This is the mechanism of quark

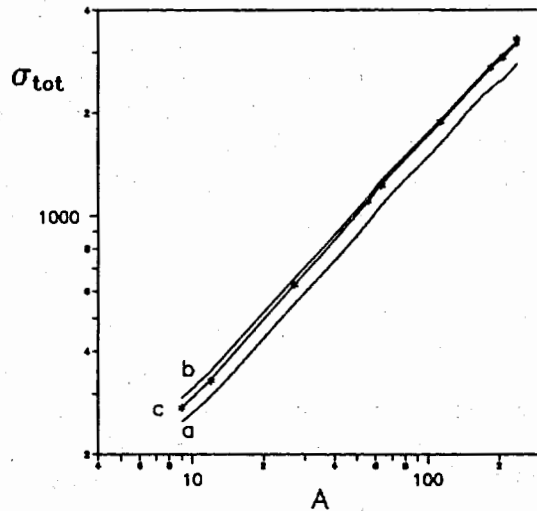


fig. 4. nA-interaction total cross section obtained with
 a) parametrization (9);
 b) the two gluon exchange approximation;
 c) parametrization (11).

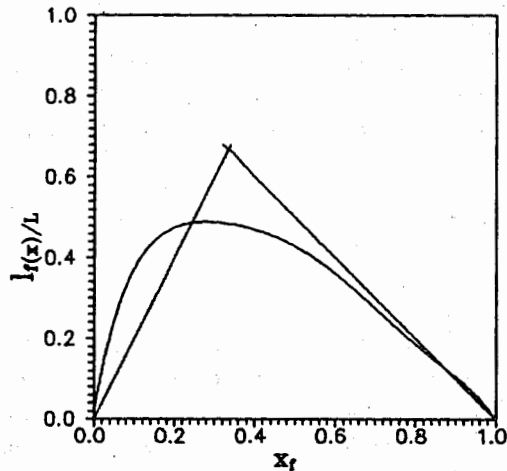


fig. 5. The x-dependence of the formation lengths: straight lines correspond to expressions (14) and (13) respectively, the curve corresponds to the constituent formation length of the LUND model from ref. (16).

hadronization^{/14/}. In the laboratory frame light fragments of the string are chipped off the leading heavy string in accordance with the chronology typical for the multiperipheral models: the higher is the particle momentum, the later it is created. The leading particle, carrying a considerable part x of the initial quark momentum, is produced last. Nevertheless, its formation zone decreases with the particle momentum and tends to zero towards $x=1$. This is a trivial consequence of the momentum conservation law. The leading hadron carrying the largest part of the initial quark momentum, should include just this quark. The latter has been continuously slowed down with a constant force independently on whether the string has been broken or interacted inside the nucleus

$$\dot{k} = -\kappa, \quad (12)$$

where κ is the string tension. The typical loss of energy 1 Fm is of about 1 GeV. The momentum of the quark placed at the fast end of the string at the moment of the latest string -breaking determines the momentum of the leading hadron. It follows from (12) that the momentum of leading hadron is

$$xk = k - \kappa l_f,$$

where l_f is the distance between the point of the incoming quark creation (interaction point) and the point of the latest breaking of the string. It has a meaning of a formation length of the leading hadron and is connected with quantities x and k by the relation^{/1,15/}

$$l_f = \frac{k}{\kappa} (1 - x). \quad (13)$$

Note that formation length of nonleading particles at small values of x does not decrease but grows up with the increasing of x :

$$l_f = 2xk/\kappa. \quad (14)$$

As the region of small x is affected considerably by cascading processes inside a nucleus, we shall restrict ourselves in what follows by the production of leading hadrons. Both expressions (13) and (14) join at $x = 1/3$ as is shown on fig.5.

These estimations are close to the results of more detailed calculations with LUND model^{/16/} (see fig.5). The latter gives one-to-one correspondence between the breaking points of the string and the momenta of final hadrons.

Now let us consider the colour - string passing the nuclear matter before the hadron has been produced. It is natural to assume, that the string, which has a length in the laboratory frame of the order or shorter than the target nucleon size, interacts at high energies like an ordinary hadron. This means, that after the string interaction two triplet strings (corresponding to the cylindrical pomeron in the dual topological model) are formed. After the interaction of the string with a bound nucleon, its slow end is thrown over to the rest diquark and the scenario is repeated from the very beginning, but the input momentum of the quark being smaller than the initial one:

$$k' = k - \kappa(z'' - z), \quad (15)$$

where z'' is the quark interaction point. So two new strings appear, as if a quark of momentum k' has been produced just in this point. The production of a hadron with momentum xk then corresponds to a new momentum fraction x'

$$x' = x \frac{k}{k - (z'' - z)}. \quad (16)$$

Though the nuclear medium does not change the formation length, it can influence the probability for production of a hadron with momentum xk . Nuclear matter distorts the effective probability (fragmentation function) of a hadron formation, which takes the form /17/:

$$D_{\text{eff}}(x, b) = D(x) \exp \left\{ - \sigma_s \int_z^{z'} dz_1 \rho(b, z_1) \right\} + \sigma_s \int_z^{z'} dz'' \rho(b, z'') D(x') \exp \left\{ - \sigma_s \int_{z''}^{z'} dz_1 \rho(b, z_1) \right\}, \quad (17)$$

where x' is given by (16), z' is the hadron formation point, σ_s is the cross section of inelastic interaction of the string with a nucleon. First term in (17) corresponds to the absence of string rescatterings within the interval $z < z'' < z'$. The second term corresponds to the situation where the last string interaction takes place at the point z'' with an arbitrary number of interactions before it and no subsequent interaction in the

interval $z' - z''$. It should be emphasized, that expression (17) takes into account all possible interactions of the string or the hadrons with the nuclear matter before production of the hadron with given momentum xk .

As has been shown in ref. /17/, the phenomenological treatment of the effective cross section of quark attenuation as an universal parameter /16/ is not correct. This cross section would depend on a mass number of a target nucleus, an energy and a string tension. Expression (17) provides a correct inclusion of the quark attenuation into nucleus interaction considerations.

5. Leading particle creation in hadron-nucleus interactions

Leading particle creation in the hadronic interactions is a result of the fragmentation of the quarks carrying a considerable part of the incoming-hadron momentum. The fragmentation starts as a consequence of the incident-hadron interaction with one of the nuclear nucleons and essentially depends on interaction's mechanism. Below, different possibilities are considered.

5.1 Cylinder-type diagram contribution

In result of a beam (for example meson) interaction with a nucleon, the projectile valence quarks form two strings together with quarks of the target nucleon. After that, strings fragmentate into hadrons, as is shown on fig.6. At large x_p values, $1 - x_p \ll 1$, this diagram corresponds to the RRP graph in regge phenomenology.

The cross section of a hadron creation with a momentum $x_p p$ is given by

$$\frac{d\sigma^{(h_1 N \rightarrow h_2 X)}}{dx_p} = \sigma_{\text{in}}^{hN} \int_{x_p}^1 \frac{dx_v}{x_v} F_{h_1}(x_v) D(x_p/x_v), \quad (18)$$

where $F(x_v)$ is the beam - hadron structure function for the quark carrying relative momentum x_v and $D(x_p/x_v)$ is the quark-to-hadron h fragmentation function. The cross section of the two strings formation is equal to the inelastic hN interaction cross section.

In the case of nuclear target the fragmentation function $D(z)$ is modified according to (17). As a result, for the hadron-nucleus cross section we get

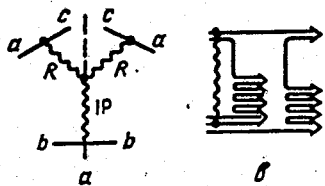


fig. 6. The cylinder-type diagram corresponding to the triple regge graph RRP.

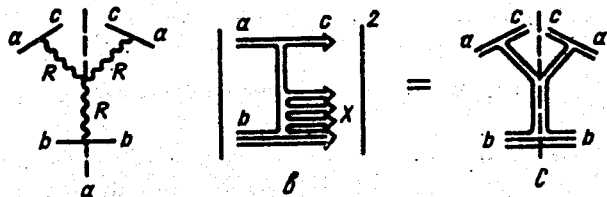


fig. 7. The planar-type diagram corresponding to the triple regge graph RRR.

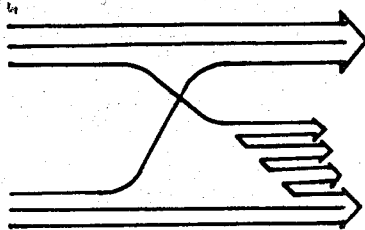


fig. 8. The planar-type diagram corresponding to the real part of the scattering amplitude.

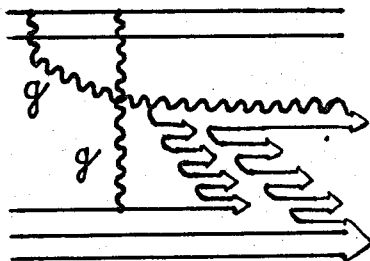


fig. 9. The triple regge graph PPP corresponding to the diffraction.

$$\frac{d\sigma^{(h_1 \rightarrow h_2 X)}}{dx_F} = A \int d^2b \int_{-\infty}^{\infty} dz \rho(b, z) \int \frac{dx_v}{x_v} F_{h_1}(x_v) \left[\frac{D(x_v/x_v)}{h_2/c} W_{h_1}(-\infty, z, b) * \right. \\ \left. W_s(z, z+l_r, b) \cdot W_{h_2}(z+l_r, \infty, b) + \sigma_s \int_z^{z+l_r} dz'' \rho(b, z'') D(x_v''/x_v) W_{h_1}(\infty, z, b) * \right. \\ \left. W_s(z'', z+l_r, b) \cdot W_{h_2}(z+l_r, \infty, b) \right]. \quad (19)$$

Here

$$W_{h_1}(-\infty, z, b) = \langle \exp \left\{ -\sigma(\rho) \int_{-\infty}^z dz_1 \rho(b, z_1) \right\} \rangle_{h_1} \quad (20)$$

is the probability of no interaction of the incident hadron till the first interaction at the point z . In expression (20) the nuclear colour transparency, i.e. inelastic shadowing, is taken into account

$$W_{h_2}(z+l_r, \infty, b) = \langle \exp \left\{ -\sigma(\rho) \int_{z+l_r}^{\infty} dz_1 \rho(b, z_1) \right\} \rangle_{h_2} \quad (21)$$

Here we suppose, that the beam and the final hadron transverse sizes are not correlated and the averaging over them can be performed independently. This assumption is justified by the fact that before the leading - hadron formation, $q\bar{q}$ - pairs are created from the vacuum with different impact - parameters within the transverse string size and the information about the hadron size is lost. By this reason (fluctuations of the distance between the quarks at the string end - points in the impact-parameter plane) the probability of no interaction of the string can be estimated as follows,

$$W_s(z_1, z_2, b) = \exp \left\{ -\sigma_s \int_{z_1}^{z_2} dz_3 \rho(b, z_3) \right\}. \quad (22)$$

Here σ_s is the effective inelastic string-interaction cross section, which is of the same order as the hadron one. In what follows, we fix $\sigma_s = \sigma_{ln}^{hN}$.

5.2. Planar-type diagrams

Planar diagram, which correspond to RRR graph in triple regge limit $x_f \rightarrow 1$, is shown on fig.7. In this case, the initial hadron antiquark is slowed down and annihilates with a target quark. The string then formed takes whole incident energy. The cross section of this process is proportional to the fragmentation function and does not essentially depend on the initial-hadron transverse size. So the contribution of the planar graph to the inclusive cross section is given by

$$\frac{d\sigma^{(h_1 A \rightarrow h_2 X)}}{dx_f} = A \int d^2b \int_{-\infty}^{\infty} dz \rho(b, z) \left[D(x_f) W_{h_1}(-\infty, z, b) W_{h_2}(z, z+l_f, b) + \sigma_s \int_z^{z+l_f} dz'' \rho(b, z'') D(x') W_{h_1}(-\infty, z, b) W_{h_2}(z'', z+l_f, b) \right] \quad (23)$$

Note, that in the reactions $pN \rightarrow pX$ or $pN \rightarrow AX$ instead of planar diagram, one shown in fig.8 is present. It corresponds to the real part of the reggeon contribution (the same contribution occurs for the diagram on fig.8). The quark fragmentation function is then $D(z) = \delta(z-1)$ and the cross section is proportional to the incoming-hadron structure function. It is interesting to note, that in this case the hadron structure function is deformed by the nuclear medium in the same way as the quark fragmentation function (section 3). Indeed, before the interaction takes place at the point z the incoming hadron could interact inelastically at some point z' . Its structure function in this case should have been harder since the leading diquark has been slowed down during passing the distance $z-z'$. The cross section is defined by the same expression (23), with $D(x)$ substituted by $F(x)$. The value of z' varies from z to $z + l_f$, where $l_f = \frac{P_0}{K}(1-x)$ (P_0 is incoming hadron momentum). However, l_f has no more the meaning of a formation length, though formally the expression remains the same.

5.3 Diffraction contribution

In the case of $h_1=h_2$ diffraction gives an essential contribution to the process cross section. Let us consider the diagram in fig.9, which corresponds to the triple-regge graph PPP. In this case, string formation and fragmentation are connected with presence of at least one sea $q\bar{q}$ - pair or gluon in the incoming hadron's wave function. The valence quarks are now in an octet colour state and should be transformed into a color singlet state in the result of interaction at a point z . This transition is suppressed by a factor $1/8$, which explains the smallness of diffraction's contribution.

In the case under consideration the formation time is zero, because all the valence quarks are spectators. Nevertheless, as in the previous case, the incoming hadron can interact inelastically at a point z_1 before the interaction at the point z . As a result, the valence quarks start losing their energy. So a share of incident momentum carrying by the valence quarks should be higher (or, equivalently, the gluon structure function must be softer) in order to compensate these losses. However, in this case the gluon structure-function softening does not lead to decreasing of the cross section if $z-z_1 \leq l_f$. Therefore the diffraction contribution to the cross section has the following form

$$\frac{d\sigma^{(h_1 A \rightarrow h_2 X)}}{dx_f} = A \int d^2b \int_{-\infty}^{\infty} dz \rho(b, z) W_{h_1}(z, z+l_f, b) \quad (24)$$

where

$$W_{h_1}(z, z+l_f, b) = \int d^2\rho |\Psi_{h_1}(\rho)|^4 \sigma(\rho) \exp\left\{-\sigma(\rho) \left[\int_{z+l_f}^z dz_1 \rho(b, z_1) + \int_{z+l_f}^{\infty} dz_1 \rho(b, z_1) \right]\right\}$$

6. Deformation of the projectile wave function by interaction with a target

We have derived expression (18) under the assumption that the incoming hadron interaction doesn't change the parton's momentum distribution in the hadron. However, the interaction cross section may depend on the parton momenta, so this assumption may not be true. Therefore, we have to use an effective structure function $\tilde{F}(x_v)$ affected by the interaction with the target instead of $F(x_v)$ (in expression (18)). Thus, in the expansion of the hadron wave function over Fock states with different numbers of sea $q\bar{q}$ -pairs, different components have essentially different quark's momentum distributions. The contribution of these components to the total cross section corresponds to graphs with different number of cut pomerons in the regge phenomenology.

The weights σ_n of this graphs in the total inelastic cross section can be estimated in the quasieikonal approximation^{/18,19/}. In fact this approximation is ungrounded for $n \geq 3$, but these terms are inessential at moderate energies. Besides quasieikonal nicely fit data on multiplicity distribution^{/19/}. The values of σ_n are formed by the weight of the corresponding Fock component of the hadron wave function which is target independent, and by the cross-section of the interaction of this component with the target. As the hadron - fluctuation interaction cross section is determined mainly by its transverse size, then the different Fock's components with close sizes, must have close cross sections. For simplicity, let us suppose their equality. As a result, we are led to the conclusion that the effective structure function

$$\tilde{F}(x_v) = \sum_{n=1}^{\infty} \sigma_n F_n(x_v) \quad (25)$$

is nearly target independent. Note that this conclusion crudely violates the AGK cutting rules^{/20/}, used in paper^{/21/} for determination of σ_n . However, in the case of nuclear target this procedure leads to an obvious puzzle: the mean number of cut pomerons grows with increasing of an atomic number. On the other hand the high-n Fock's components of the projectile hadron wave function should be strongly suppressed, and their tiny weights cannot be compensated by the interaction probability, which is under unity. It can be argued that the AGK rules does not work in

QCD¹. Therefore, in what follows the same weights σ_n are used for both nuclear and nucleon targets.

7. The results of calculations and comparison with experimental data

To calculate the cross sections for the secondary - particle production, it is necessary to know the momentum distribution of projectile quarks and their fragmentation functions. We shall use the structure and fragmentation functions obtained in framework of the quark-gluon string model (QGSM). This model is based on the idea of QCD 1/N - expansion in the framework of the dual topological -unitarization scheme. In the QGSM structure - and fragmentation - functions are defined by their regge behaviour^{/22,23/} in the limits $x \rightarrow 0$ and $x \rightarrow 1$, and by simple interpolation formulae in the intermediate x-region. These functions satisfy the momentum, charge, baryon-number and strangeness conservation laws^{/24/}. The effective structure functions $\tilde{F}_n(x_v)$ for protons are given by

$$\begin{aligned} \tilde{F}_{uu}(x,n) &= C_{uu}^{(n)} x^{\alpha_R - 2\alpha_B + 1} (1-x)^{-\alpha_R + n - 1} \\ \tilde{F}_{ud}(x,n) &= C_{ud}^{(n)} x^{\alpha_R - 2\alpha_B} (1-x)^{-\alpha_R + n - 1} \end{aligned} \quad (26)$$

where $\alpha_R \equiv \alpha_R(0)$ and $\alpha_B \equiv \alpha_B(0)$ are the intercepts of the leading reggeon and baryon trajectories respectively, which take the values $\alpha_R \approx 0,5$ and $\alpha_B \approx -(0,4 - 0,5)$.

For the π^+ - meson and K^+ - meson respectively we shall use the following distributions

$$\begin{aligned} F_u(x,n) = F_d(x) &= C_u^{(n)} x^{-\alpha_R} (1-x)^{-\alpha_R + n - 1} \\ F_s(x,n) &= C_s^{(n)} x^{-\alpha_\phi} (1-x)^{-\alpha_R + n - 1} \end{aligned} \quad (27)$$

$$F_s(x,n) = C_s^{(n)} x^{-\alpha_\phi} (1-x)^{-\alpha_R + n - 1} \quad (28)$$

with $\alpha_\phi \approx 0$. Coefficients $C_i^{(n)}$ in (27), (28) are determined by the normalization condition

¹This point is a subject of a separate paper by B.G.Zacharov and one of the authors (B.Z.K.).

$$\int F_1(x_v, n) dx_v = 1 \quad (29)$$

The weight coefficients σ_n in expression (25) are calculated in the quasieikonal approximation^{18,19/}.

The fragmentation functions of quarks and diquarks into final baryons are given by^{24,25/}

$$D_{ud}^p(z) = a_N \frac{1}{z} z^{2(\alpha_R - \alpha_B)} (1-z)^{\lambda - \alpha_R} (1-0.48z) \quad (30)$$

$$D_{uu}^p(z) = a_N \frac{1}{z} z^{2(\alpha_R - \alpha_B)} (1-z)^{\lambda - \alpha_R} (2.48 - 1.96z) \quad (31)$$

$$D_{ud}^\Lambda(z) = a_\Lambda \frac{1}{z} z^{2(\alpha_R - \alpha_B)} (1-z)^{\lambda - \alpha_\phi} \quad (32)$$

$$D_{uu}^\Lambda(z) = a_\Lambda \frac{1}{z} z^{2(\alpha_R - \alpha_B)} (1-z)^{\lambda - \alpha_\phi + 1} \quad (33)$$

where $\lambda = 2\langle p_t^2 \rangle \alpha'_R(0) = 0.3 - 0.5$.

The quark-into-meson fragmentation functions have the following form :

$$D_u^{\pi^+}(z) = a_\pi \frac{1}{z} (1-z)^{\lambda - \alpha_R} (1+0.84z(1-z)-0.85z) \quad (34)$$

$$D_s^{\kappa^0}(z) = a_\kappa \frac{1}{z} z^{-\alpha_\phi} (1-z)^{\lambda - \alpha_R} (1-0.7z)(6.8-5.2z) \quad (35)$$

Let us consider the leading-hadron production in hadron-nucleus inelastic interactions.

7.1. Process $hA \rightarrow hX$

At high energies we can restrict ourselves by the scaling contributions of the diagrams shown on figs.7,10. The relative contributions of these two mechanisms at each value of x have been specified by an approximation of the hadron proton invariant inclusive cross - section data using the parameterization from ref.^{26/}. The cross sections have been calculated with the help of expressions (19) and (24) respectively. In the averaging over the transverse hadron size parameterization (11) has been used for $\sigma(\rho)$. The inelastic cross section σ_s for string interaction with the nucleus has been assumed to be equal to the inelastic cross section of the initial hadron.

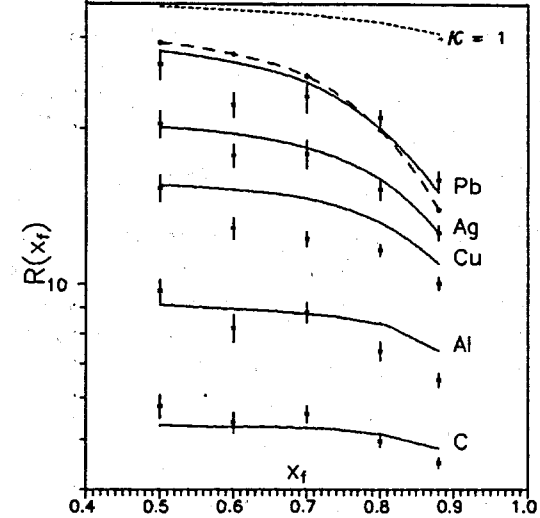


fig. 10. Ratios of the differential cross sections $R_A = \frac{d\sigma}{dx}(pA \rightarrow pX) / \frac{d\sigma}{dx}(pp \rightarrow pX)$ at 100 GeV. Solid curves represent our predictions, the dashed curve - calculations without inelastic corrections, the dotted curve - calculations with a string tension constant $\kappa = 1$ GeV/fm.

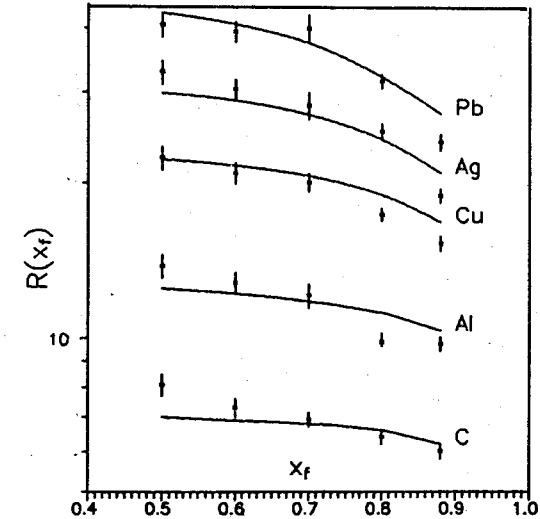


fig. 11. Ratios of the differential cross sections $R_A = \frac{d\sigma}{dx}(\pi A \rightarrow \pi X) / \frac{d\sigma}{dx}(\pi p \rightarrow \pi X)$ at 100 GeV.

Here we consider the string tension coefficient κ as a free parameter. Its value may be different from the static string one ($\kappa = 1 \text{ GeV/fm}$). This difference reflects the fact that the coloured objects are slowed down not only by the string tension, but also by the gluon bremsstrahlung after colour is exchange^{/33/}. The latter leads to an effective increase in κ . The value of κ has been determined from the best description of the experimental data. Thus, in all investigated processes the colour - string tension coefficient is fixed at $\kappa = 3 \text{ GeV/fm}$. We note that this value agrees with those obtained from the data on large- p_t hadron pair production^{/3/} and J/ψ hadroproduction on nuclei^{/2/}.

The results for the relative inclusive cross section ratio

$$A_{\text{eff}}(x) = \frac{d\sigma^{\text{hA}}}{dx} / \frac{d\sigma^{\text{hp}}}{dx} \quad (36)$$

for processes $p + A \rightarrow p + X$ and $\pi + A \rightarrow \pi + X$ at $100 \text{ GeV}^{/27/}$ are represented in fig.10 and in fig.11 respectively, both showing a good agreement with the experimental data. Note that the decreasing of $A_{\text{eff}}(x)$ with the increasing of x is well reproduced, just because the leading hadron formation length has been taken into account.

7.2. Process $pA \rightarrow \Lambda X$

In this process there are no RRR- and PPP- type diagrams. The inclusive cross sections is entirely determined by the cylindrical-type diagram (RRP). The ratios Pb/Cu of the cross sections of inclusive Λ - production at energy $400 \text{ GeV}^{/28/}$ is shown in fig.12. For $x > 0,9$ the theoretical curve sharply decreases in disagreement with the experimental data. This is a surprising result as the same approach nicely fits the data on reaction $pA \rightarrow pX$ at 100 GeV having very similar dynamics. Below we discuss possible sources of disagreement, but anyway new experimental data at $x > 0,9$ both on nuclear and hydrogen targets would be desired.

7.3. Process $\pi^+ A \rightarrow pX$

Both cylindrical RRP, planar RRR diagrams are valuable for this process. It is easy to estimate the contribution of each of them from comparison of the experimental cross sections of the processes $\pi^+ p \rightarrow pX$ and $\pi^- p \rightarrow \bar{p}X$. The latter cross section is

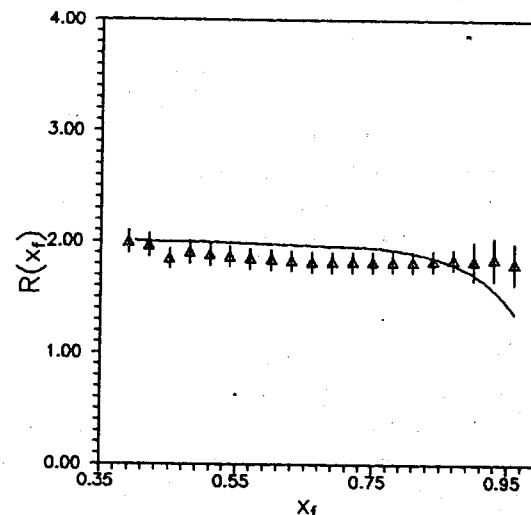


fig. 12. Ratio of the differential cross sections $R_A = \frac{d\sigma}{dx}(\text{pPb} \rightarrow \Lambda X) / \frac{d\sigma}{dx}(\text{pCu} \rightarrow pX)$ at 400 GeV .

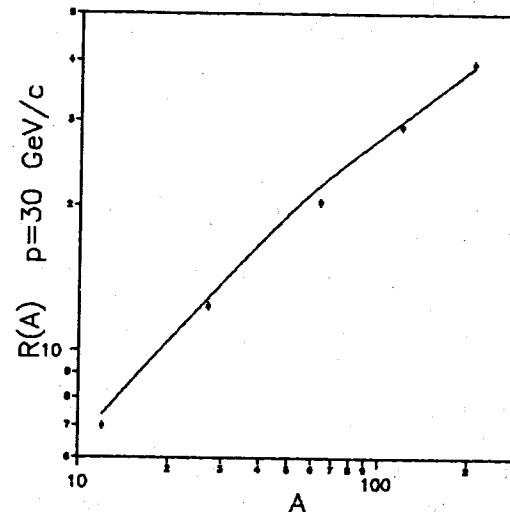


fig. 13. The inclusive cross section ratios $\sigma(\pi^+ A \rightarrow pX) / \sigma(\pi^+ p \rightarrow pX)$ at 30 GeV for $x_f = 0.5$

entirely determined by the cylinder-type diagram. Thus, the contribution of the planar-type diagram is given by

$$\sigma^{p1} = \sigma^{\pi^+ \rightarrow p} - \sigma^{\pi^- \rightarrow \bar{p}}.$$

The ratio A_{eff} for the process $\pi^+ A \rightarrow pX$ at an energy of 30 GeV^{/29/} ($x_f = 0.5$) as a function of the target nuclear mass number A (C,Al,Cu,Sn and Pb) is shown on fig.13, together with the theoretical predictions. The model calculations are in a good agreement with the experimental data.

7.4. Processes $K^+ A \rightarrow K^0 (K^{*0}) X$

The scaling diagrams of the cylinder-type give the main contribution^{/30,31/} to the cross sections of these processes. The cross section ratios have been calculated with the help of eq. (19). The results are presented on fig.14 in comparison with the experimental data on inclusive creation of K^0 - and K^{*0} - mesons at 11 GeV^{/32/}. The ratios for K^0 - and K^{*0} - mesons ($R(\text{Cu}/\text{Be})$) and for K^{*0} - mesons ($R(\text{Pb}/\text{Be})$) are in a good agreement with the experimental data. The reason for the relatively lower experimental values of $R(\text{Pb}/\text{Be})$ for K^0 - mesons is still an open question.

8. Discussions

In this paper we have developed an approach to the soft hadron- nucleus interactions, incorporating our understanding of the QCD induced dynamics of strong interactions. We have made an effort to take into account both the space-time pattern of particle production and inelastic corrections to the eikonal approximation. The latter have been estimated in the QCD motivated manner, taking into account the effects of the nuclear colour transparency. Attenuation of quarks at an early stage of particle production has also been included. We have described a bulk of data on particle production in the projectile fragmentation region. The latter was chosen in order to enhance the effects of formation time and to eliminate the influence of cascading in the nucleus. The typical manifestation of QCD predicted behaviour of formation length is the fall off of the nucleus to proton ratios

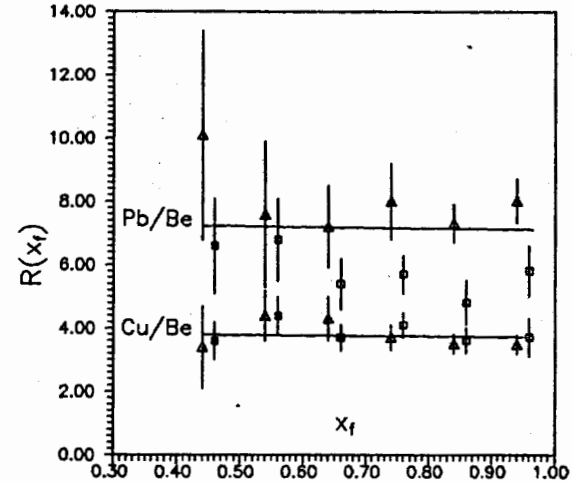


fig. 14. Ratios of differential cross sections $\frac{d\sigma}{dx}(K^+ A \rightarrow K^0 X) / \frac{d\sigma}{dx}(K^+ \text{Be} \rightarrow K^0 X)$ and $\frac{d\sigma}{dx}(K^+ A \rightarrow K^{*0} X) / \frac{d\sigma}{dx}(K^+ \text{Be} \rightarrow K^{*0} X)$ at 11,2 GeV.

of inclusive cross section towards $x_f=1$. Note that decreasing of this ratio was also predicted in the approach^{/21/}, where considerable softening of the projectile parton distribution by a nucleus was suggested in accordance with the AGK cutting rules, but in the same time the formation length of all produced hadrons was assumed being much larger than the nucleus radius without any motivation. On the contrary, we accounted correctly the latter and argued the invalidity of AGK rules for nuclei.

The 100 GeV data on $pA \rightarrow pX$ reaction nicely agree with the predicted behaviour of inclusive spectra, whereas analogous data on reaction $pA \rightarrow AX$ at 400 GeV show no decrease of cross section up to $x_f=0.96$. Considering both data being correct one should discuss a possible way out of this dramatic contradiction. The discrepancy with A production data would vanish, if one decreased the value of string tension for instance to $\kappa \approx 1\text{GeV}/\text{Fm}$. In this case the computed ratio of cross sections in fig.12 would bend over at higher x_f . On the other hand the decrease of κ would lead to overestimation of the 100 GeV data at moderate x_f values. At this moment it would be possible to turn on other reserves. In fact we an oversimplified situation assuming the no influence of a nuclear

target on the parton distribution. Some softening effect should exist of course, and it would suppress the inclusive cross section ratio. Another possible source of diminution of this ratio is an additional attenuation of diquark in nuclear matter during the formation time due to possibility of its destruction by means of conversion to a sextet colour state^{/34,35/}. This correction may be essential for both p and Λ production reactions.

Acknowledgements

We have greatly benefited from discussions with B.G.Zakharov of all subjects concerned in this paper.

References

1. Kopeliovich B.Z., Lapidus L.I., Proc. of the VI Balaton Conference on Nucl. Phys., p.73, Balatonfured, Hungary, 1983
2. Kopeliovich B.Z., Niedermayer F., JINR preprint E2-84-834, Dubna, 1984
3. Kopeliovich B.Z., Niedermayer F., Yad. Fiz., v.42, (1985) 797
Kim V.T., Kopeliovich B.Z., JINR preprint E2-89-727, Dubna, 1989 (to be published in Z. Phys. C).
4. Glauber R.J., High Energy Collision Theory, v.1, p.315, Inter-science Publisher, 1959
5. Sitenko O.G., Ukraj.J.of Phys., v.4, (1959) 152
6. Gribov V.N., J. Exp. Theor. Phys., v.56, (1969) 892
Gribov V.N., in: Proceedings of the VIII. Winter School LINF - Leningrad, v.2, (1973) 5
7. Karmanov V.A., Kondratjuk L.A., The Letters in Exp. and Theor. Phys. J., v.18, (1973) 451
8. Kopeliovich B.Z., Lapidus L.I., The fifth international workshop of multihadron production at high energies, Dubna, (1978) 469
9. Good M.L., Walker W.D., Phys. Rev., v.120, (1960) 1857
10. De Jager C.W., De Vries H., De Wries C., Nuclear Data Tables, v.36, N3, (1987) 495
11. Nikolaev N.N., preprint INS - REP - 538, (1985)
12. Murthy P.V.R. et al., Nucl. Phys., B92, (1975) 269
13. Gotsman E., Nussinov S., Phys. Rev., D22, (1980) 624
Migdal A. B., Sov. Phys. JETP, Lett. 46, (1987) 256

14. Casher A., Neuberger H., Nussinov S., Phys. Rev., D20, (1979) 179
15. Kopeliovich B.Z., Niedermayer F., Sov. J. Nucl. Phys., v.42, (1985) 504
16. Bialas A., Gyulassy M., Nucl. Phys., B291, (1987) 793
17. Kopeliovich B.Z., JINR preprint E2-90-175, Dubna, 1990 (to be published in Phys. Lett. B)
18. Volkovitsky P.E. et al., Yad. Fiz., v.24, (1976) 1237
19. Ter-Martirosyan K. A., Phys. Lett., B44, (1973) 377
20. Abramovsky V.A., Gribov V.N., Kancheli O.V., Yad. Fiz., v.18, (1973) 595
21. Kaidalov A.B., Ter-Martirosyan K.A., Shabelski Yu.M., Yad. Fiz., v.43, (1986) 1282
Shabelski Yu.M., Yad. Fiz., v.45, (1987) 223
22. Kaidalov A.B., Phys. Lett., B116, (1982) 459
Kaidalov A.B., Ter-Martirosyan K.A., Phys. Lett., B117, (1982) 247
Kaidalov A.B., Ter-Martirosyan K.A., Yad. Fiz., v.39, (1984) 1545
Kaidalov A.B., Ter-Martirosyan K.A., Yad. Fiz., v.40, (1984) 211
Kaidalov A.B., Yad. Fiz., v.33, (1981) 1369
23. Kaidalov A.B., Yad. Fiz., v.45, (1987) 1452
24. Shabelski Yu.M., Yad. Fiz., v.44, (1986) 186
25. Kaidalov A.B., Piskunova O.I., Z. Phys, C30, N^o=1, (1986) 145
26. Kazarinov Yu.M., Kopeliovich B.Z., Lapidus L.I., Potashnikova I.K., J. Exp. Theor. Phys., v.70, (1976) 1152
27. Barton D.S. et al., Phys. Rev., D27, (1983) 2580
28. Beretvas .et al., Phys. Rev., D34, (1986) 53
29. Abreu M.G. et al., Z. Phys., C25, (1984) 115
30. Zakharov B.G., Sergeev V.N., Yad. Fiz., v.30, (1979) 236
31. Zakharov B.G., Sergeev V.N., Yad. Fiz., v.39, (1984) 920
32. Akimenko S.A. et al., IHEP preprint 90-10, Serpuchov, 1990
Akimenko S.A. et al., IHEP preprint 90-31, Serpuchov, 1990
33. Niedermayer F., Phys. Rev., D34, (1986) 3494
34. Kopeliovich B.Z., Zakharov B.G., Yad. Fiz., v.49, (1989) 1087
35. Kopeliovich B.Z., Zakharov B.G., Z. Phys., C43, (1984) 241

Received by Publishing Department
on May 24, 1990.

Копелиович Б.З., Литов Л.Б., Немчик Я.
Эффекты времени формирования и цветовой
прозрачности при рождении лидирующих частиц
на ядрах

E2-90-344

Образование лидирующих частиц в адрон-ядерных взаимодействиях при высоких энергиях свободно от ядерных каскадов и является чувствительным к зависимости длины формирования от импульса частиц. Кроме того, эти процессы чувствительны и к неупругим поправкам, которые делают ядро более прозрачным. Это дает возможность также проверить предсказание КХД о цветовой прозрачности ядра, которое является частным случаем неупругого затемнения. Мы предлагаем подход учета этих эффектов, основанный на дуальной струнной модели. Проводится сравнение предсказаний модели с широким классом инклюзивных адрон-ядерных процессов. Обнаружено хорошее совпадение с экспериментом.

Работа выполнена в Лаборатории ядерных проблем ОИЯИ.
Препринт Объединенного института ядерных исследований. Дубна 1990

Kopeliovich B.Z., Litov L.B., Nemchik J.
Effects of Formation Time and Colour Transparency
in the Production of Leading Particles Off Nuclei

E2-90-344

Production of the leading particles in hadron-nucleus interactions at high energies is free from the nuclear cascading influence and is most sensitive to the formation time dependence on the particle momentum. Besides, these processes are sensitive to the inelastic corrections which make nuclei more transparent. This provides also a possibility to test the QCD prediction on the nuclear colour transparency, which is only a special case of the inelastic shadowing. We develop an approach based on the dual string model and taking into account all these effects. We test it on a bulk of data and obtain a nice agreement.

The investigation has been performed at the Laboratory of Nuclear Problems, JINR.

Preprint of the Joint Institute for Nuclear Research. Dubna 1990